Sensor networks

Expansion of Measurement Range of Low-Cost Ethernet-Based Temperature Sensing System Using Long-Period Fiber Grating

Shogo Nanataki, Osanori Koyama, Kei Narumiya, Kanami Ikeda, and Makoto Yamada

Department of Electrical and Electronic Systems Engineering, Osaka Metropolitan University, Sakai 599-8531, Japan

Manuscript received 15 November 2023; revised 12 December 2023; accepted 13 December 2023. Date of publication 18 December 2023; date of current version 29 December 2023.

Abstract—It is important to reduce the cost of the sensing system to promote the social implementation of optical fiber sensors. The light source and the photodetector with analysis functions, e.g., optical spectrum analyzer, are the most expensive components of an optical fiber sensing system. To solve this problem, we have proposed an Ethernet-based temperature sensing system. This system uses an inexpensive optical transceiver (OTR) as a light source for the Ethernet and a photodetector and a single-board computer with temperature evaluation functions to reduce the system cost. In this letter, we propose a method to enhance the temperature sensing function in our proposed Ethernet-based temperature sensing system by using multiple OTRs with different output wavelengths and an optical switch to expand the measurement temperature range. In addition, we constructed the proposed system and conducted a demonstration experiment to expand the temperature range that can be measured using five OTRs, one optical switch, Raspberry Pi, and a long-period fiber grating as an optical fiber sensor. The experimental results show that the temperature range from 60 to 760 °C can be expanded with an error of approximately ±5 °C.

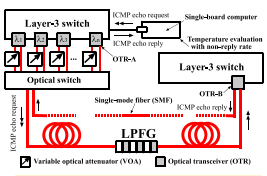

Ethernet-based temperature sensing system using long-period fiber grating

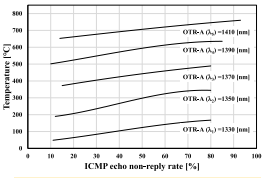

Expansion of measurement range by adding Ethernet optical transceivers

Index Terms—Sensor networks, ethernet, long-period fiber grating, optical fiber sensing, single-board computer, temperature sensing system.

I. INTRODUCTION

Compared with electrical sensors, optical fiber sensors possess several advantages, including features, such as not requiring a power supply to activate the sensing device, immunity to electromagnetic interference, the ability to measure over long distances without optical amplifiers, robustness, and high reliability in the face of environmental changes. Long-period fiber grating (LPFG) is one type of optical fiber sensor device. LPFGs attenuate specific wavelengths of light in the core of an optical fiber. These specific wavelengths are referred to as resonance wavelengths, and LPFGs exhibit the unique property of shifting in response to changes in various environmental parameters surrounding the LPFG [1]. By measuring the amount of the shift, numerous methods have been proposed for sensing environmental parameters, such as temperature [2], [3], [4], strain [5], [6], and the refractive index of liquids [7], [8].

However, the cost of components that make up an optical fiber sensing system, especially broadband light sources and optical spectrum analyzers (OSAs) equipped with analytical capabilities, is generally high. This cost factor can sometimes make optical fiber sensing systems less competitive than electrical sensing systems from a cost perspective. Furthermore, the involvement of requirements for precision measurements or multipoint measurements can lead to even higher costs, often resulting in the preference for electrical sensor systems. Therefore, it is important to reduce the overall cost of the entire optical fiber sensing system to promote the societal implementation of optical fiber sensing.

Substituting low-cost equipment for broadband light sources and OSAs is one effective approach to reduce the cost of optical fiber sensing systems. As one of the cost reduction methods, we have proposed an optical fiber temperature sensing system that utilizes low-cost Ethernet optical transceivers (OTRs) as replacements for broadband light sources and OSAs [9], [10]. In addition, several research studies have been conducted on cost reduction in optical sensing schemes, such as edge filtering [11], [12]. Our proposed system is designed to operate by equipping OTRs on unused ports of Internet Protocol (IP) packet exchanging devices in existing IP networks. When purchasing new packet exchanging devices for the proposed system, it is possible that the proposed system may not be economically advantageous compared to the edge filter schemes. However, when scaling up, the proposed system, requiring only additional optical transceivers, can reduce additional system construction load and costs. Given the widespread adoption of IP networks globally, we believe that the cost-effectiveness of our proposed system remains intact, thereby offering even greater economic advantages.

In this letter, we propose a method to expand the measurement temperature range by using an optical switch and multiple OTRs with different output wavelengths to further enhance the functionality of a low-cost Ethernet-based optical fiber temperature sensing system [9]. We report the results of demonstration experiments with our laboratory system, consisting of one optical switch, five OTRs with different output wavelengths, an opposing OTR, and a single-board computer for temperature evaluation.

II. EXPANSION OF MEASUREMENT TEMPERATURE RANGE USING OPTICAL SWITCH AND OTRS WITH DIFFERENT WAVELENGTHS

In the proposed Ethernet-based optical fiber temperature sensing system [9], the temperature around the LPFG is measured by using

Corresponding author: Osanori Koyama. (e-mail: koyama@omu.ac.jp).
Associate Editor: Flavio Esposito.
Digital Object Identifier 10.1109/LSENS.2023.3344105

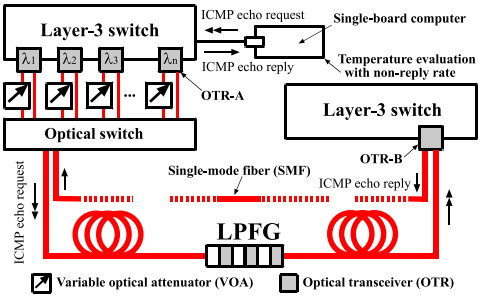

Fig. 1. Ethernet-based temperature sensing system with LPFG.

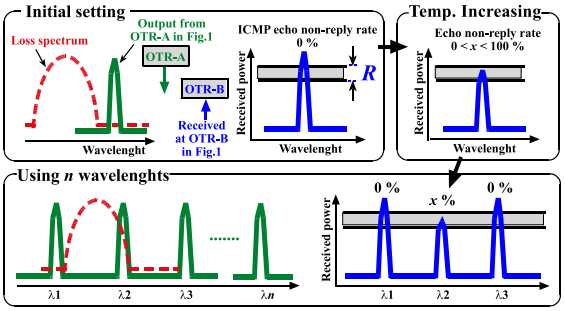

Fig. 2. Temperature sensing mechanism by using LPFG and OTRs.

the characteristic of the LPFG's optical loss spectrum shifting toward longer wavelengths with increasing temperature. By using OTRs with output wavelengths corresponding to the peak of the optical loss spectrum, the decrease in the received optical power of the receiving-side OTR with increasing temperature is correlated with the IP packet reception failure rate in the IP network. Such correlation allows for the evaluation of the temperature around the LPFG. The measurement temperature range of the proposed system was approximately 90–190 °C. OTRs with an output wavelength of 1310 nm were used in the experimental configuration in the study of Koyama et al. [9], resulting in a measurement range of about 100 °C per wavelength.

In this study, we aim to expand the measurement temperature range of the Ethernet-based optical fiber temperature sensing system using multiple OTRs with wavelengths >1330 nm, following the coarse wavelength division multiplexing (CWDM) standard. OTRs that comply with CWDM standard wavelengths are used since they are cost-effective products with wavelengths other than 1310 and 1550 nm, maintaining the low-cost of the proposed system.

Fig. 1 shows the proposed Ethernet-based temperature sensing system, which uses an optical switch and OTRs with multiple wavelengths. The system is designed to operate on an existing IP network and uses routers or layer-3 switches (L3SWs), which can exchange IP packets. Multiple Ethernet OTRs (OTRs-A) with different wavelengths are installed on L3SW ports. The number of wavelengths used is denoted as n, as shown in Fig. 1. Variable optical attenuators (VOAs) are connected to the output ports of the OTR-As to adjust the optical power output. LPFGs are used as optical fiber sensors. An optical switch can be introduced to selectively connect multiple OTRs to the LPFG. The LPFG is placed at the location of temperature measurement and is connected to the optical switch and an opposing OTR (OTR-B) through single-mode fiber (SMF). The OTR-A and OTR-B exchange Internet control message protocol (ICMP) echo request and reply packets [13] with each other for temperature evaluation.

Fig. 2 illustrates the temperature sensing mechanism in this system. Before initial setting, it is necessary to thoroughly investigate the shape

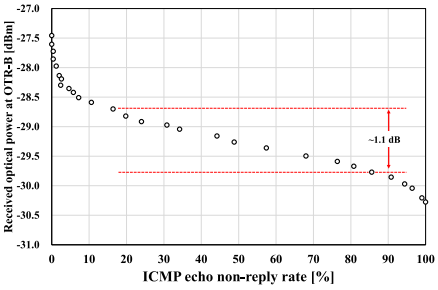

Fig. 3. OTR-B received power and ICMP echo nonreply rate.

and temperature characteristics of the optical loss spectrum of the LPFG, and determine the temperature measurement range. The top-left part of Fig. 2 displays the power spectrum of the output light from the OTR-A and the optical loss spectrum of the LPFG in the initial setting. In the initial setting, the LPFG minimally affects the output light from the OTR-A. Therefore, the VOA is used to adjust the received optical power of the OTR-B to the upper limit of the sensing region R, as shown in Fig. 2. The right-side L3SW shown in Fig. 1 can successfully receive ICMP echo request packets sent from a single-board computer via OTR-A and OTR-B and respond with ICMP echo reply packets. The single-board computer can also receive ICMP echo reply packets, which leads to an ICMP echo nonreply rate to become 0%. In this letter, we use LPFGs fabricated by irradiating commercially available SMFs for communication with CO_2 laser in the study of Murakami et al. [14]. As the temperature around the LPFG increases from the initial setting, the attenuation band of the optical loss spectrum of the LPFG shifts toward longer wavelengths. As the shift progresses, the output light from the OTR-A gradually experiences a more significant optical loss. Consequently, as shown in the upper right part of Fig. 2, the received optical power of the OTR-B gradually decreases, leading to an increase in the nonreply rate because the L3SW cannot accurately recognize the optical digital signals. Through this mechanism, it is possible to relate the temperature change around the LPFG and the shift amount of the loss spectrum of LPFG and the received optical power of the OTR-B and the nonreply rate. It is also possible to evaluate the ambient temperature of the LPFG by monitoring the nonreply rate. Furthermore, we show a method to expand the measurement range of temperature by using multiple OTR-As with different output wavelengths. The lower figure in Fig. 2 shows the case of using n wavelengths. Even if the ambient temperature of the LPFG continues to rise and the nonreply rate of λ_2 reaches 100%, it is possible to measure a new temperature range by using wavelength λ_3. The more wavelengths are multiplexed, the more the measurement temperature can be expanded.

Fig. 3 shows the relationship between the nonreply rate and the received optical power of the OTR-B used in this study, which was obtained using OTR-A, OTR-B, and VOA, without using LPFG. The nonreply rate reaches 100% when the received optical power of the OTR-B reaches the lower limit of the sensing region R. Using this mechanism, temperature can be correlated with the packet exchange performance in the IP network over the Ethernet, and temperature around the LPFG can be measured by monitoring the nonreply rate. In this letter, we adopted the range of about 15%–85% of nonreply rate as the sensing region R. In this case, R is about 1.1 dB.

Furthermore, the continuous rise in temperature corresponds to a continuous measurement in temperature as the LPFG affects the output power of OTR with longer output wavelength. When the nonreply rate reaches ~90%, the OTR-A connected to the LPFG is changed to a neighbor OTR-A with a longer output wavelength by using an optical

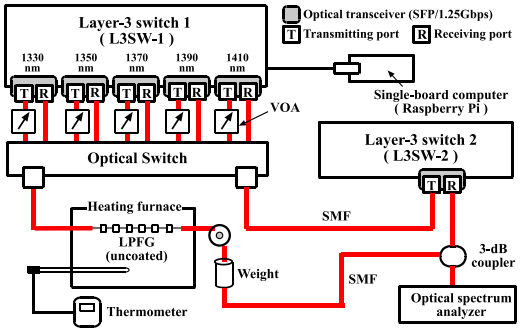

Fig. 4. Experimental setup.

switch. By changing the OTR-A, the received power of the OTR-B again exceeds the upper limit of the sensing region R. Similarly, the VOA is used to adjust the received power of the OTR-B to be at the upper limit of the sensing region R, and the nonreply rate is set again to a value near 0%. By repeating this process n times, the measured temperature range can be expanded roughly n times compared to using a single OTR-A. In this letter, OTR-As with five different output wavelengths (1330, 1350, 1370, 1390, and 1410 nm) were used.

III. EXPERIMENT AND DISCUSSION

Demonstration experiments were conducted to expand the measurement temperature range using an optical switch and OTR-As for the Ethernet with multiple wavelengths. Fig. 4 shows the experimental setup. The features of the OTRs used were compliant with small form-factor pluggable, and included an uncooled CWDM-rated distributed-feedback laser transmitter with a transmission bit rate of 1.25 Gbps. The costs of an optical switch and an OTR used were about \$860 and \$65, respectively. As an equipment for IP routing, L3SW-1 was equipped with OTR-As with output wavelengths of 1330, 1350, 1370, 1390, and 1410 nm, while L3SW-2 was equipped with an OTR-B with an output wavelength of 1310 nm. SMF was used to connect the transmitting port of the OTR-A in L3SW-1, the VOA, the optical switch, the LPFG without coating inside the heating furnace, and the receiving port of the OTR-B in L3SW-2. A 3 dB coupler and OSA were added to the experimental system to measure the optical power at the OTR-B receiving port. Thermocouple thermometer was used to measure the temperature inside the furnace. A single-board computer (Raspberry Pi) was used to generate ICMP echo packets and calculate ICMP echo nonreply rates.

In this experiment, the measurement temperature range was set from 60 to 760 °C, and the measurements were conducted using the linear range of the relationship between OTR-B's received power and ICMP echo nonreply rate, which is approximately 15%–85%, as shown in Fig. 3. When the temperature inside the heating furnace reached 60 °C, the nonreply rate was adjusted to 15% using the VOA. Initially, the OTR-A with an output wavelength of 1330 nm was used. Subsequently, the temperature inside the heating furnace was raised to 800 °C at a rate of approximately 3 °C/min. When the nonreply rate exceeded about 80%, the 1350 nm OTR-A was connected to the LPFG using the optical switch, and the nonreply rate was again adjusted to 20% using the VOA. While the temperature inside the heating furnace was rising, the Raspberry Pi was continuously pinged to monitor the nonreply rate concerning temperature. The nonreply rate was calculated from the number of nonreplies to 100 ICMP echo request packets at each temperature.

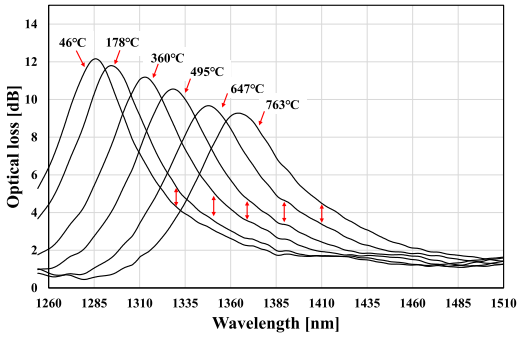

Fig. 5. Temperature dependence of the optical loss spectrum of the LPFG.

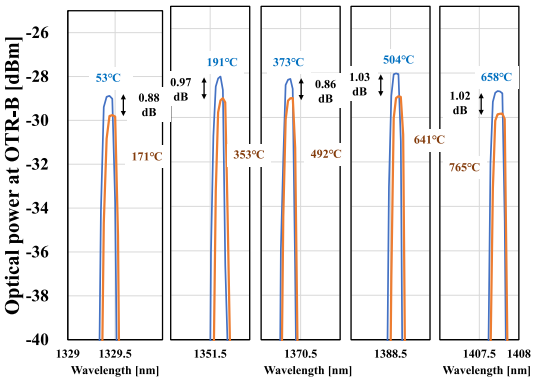

Fig. 6 Variation in the received power at the OTR-B.

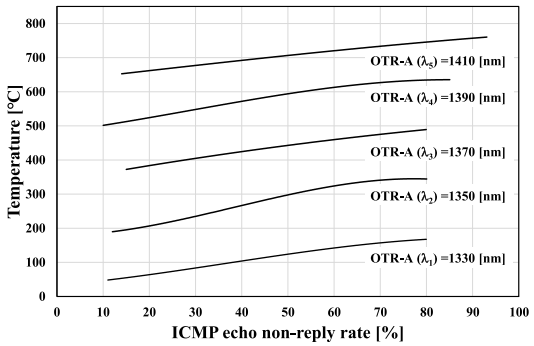

Fig. 7. Relationship between ICMP echo nonreply rate and temperature in a heating furnace.

Fig. 5 shows the temperature dependence of the optical loss spectrum of the LPFG used in this experiment. Each spectrum was measured at the starting temperature, the temperatures when switching OTR-As, and the ending temperature. It was confirmed that as the temperature around the LPFG increased, the optical loss spectrum shifted toward longer wavelengths at a rate of 0.11 nm/°C.

Fig. 6 shows the received power spectrums of the OTR-B at the start (solid lines) and end (dotted lines) of measurements for each wavelength. The decrease in the received power for the OTR-A with a wavelength of 1330 nm was close to 0.9 dB, which is within the sensing region shown in Fig. 3. This confirms that the shift in the optical loss of the LPFG affected the received power of the OTR-B.

Fig. 7 shows the relationship between the ICMP echo nonreply rate and the temperature in the heating furnace measured by the thermocouple thermometer shown in Fig. 4. A third-order polynomial

approximation curve was obtained from all data collected in the experiment. By investigating the approximation curve beforehand, it is possible to estimate the temperature around the LPFG from the ICMP echo nonreply rate calculated from the Raspberry Pi. The difference between the approximation curve and the temperature obtained from the thermocouple thermometer inside the heating furnace temperature was within the range of about ±5 °C, and the average and the standard difference were 0.40 and 2.28 °C, respectively. The difference is roughly equivalent to the difference shown in paper [9]. To enhance the precision of measurements, it is necessary to improve the experimental setup by investigating the fluctuations in optical power attributable to the optical chain. In Fig. 7, there are temperature regions that could not be measured between the adjacent approximation curves, which is caused by the increase of the furnace temperature during the manual setting of the OTR-A and the VOA and the switching of the optical switch. However, we could measure 89.8% of the total measurement range of from 60 to 760 °C. This problem can be solved by implementing an automatic setting function on the single-board computer.

The measurement accuracy of the proposed system is not as high as commercially available temperature sensors using fiber Bragg grating, which have accuracies of ±1.5 °C [15] and ±1 °C [16], respectively. However, it offers significant advantages in constructing a low-cost optical fiber sensing system capable of measuring a wide temperature range, including temperatures near 800 °C [17], which is the temperature measurement limit for the LPFGs we fabricated. In addition, it is assumed that the ability to change the measurement range by altering the output wavelength of the OTRs also makes it applicable to subfreezing temperature ranges. These features indicate the proposed system may be applicable for temperature monitoring in harsh environments. Furthermore, when applied to extensive monitoring systems with numerous measurement locations, the proposed system can easily scale by adding additional OTRs, providing a greater cost advantage compared to existing optical fiber sensing systems. We believe that the advantages of the proposed system can substantially contribute to the societal implementation of optical fiber sensing systems.

IV. CONCLUSION

We proposed a method using an optical switch and several OTRs that output multiple different wavelengths to expand the temperature measurement range of the low-cost Ethernet-based optical fiber temperature sensing system with LPFG. As a result of the demonstration experiment, we succeeded in measuring a wide range of temperatures from 60 to 760 °C, although a measurement error of about ±5 °C was observed. In the future, we plan to focus on further extending the measurement temperature range, particularly targeting subfreezing temperatures.

ACKNOWLEDGMENT

This work was supported by JSPS KAKENHI under Grant JP22K04143.

REFERENCES

[1] A. M. Vengsarkar, P. J. Lemaire, J. B. Judkins, V. Bhatia, T. Erdogan, and J. E. Sipe, "Long-period fiber gratings as band-rejection filters," *J. Lightw. Technol.*, vol. 14, no. 1, pp. 58–65, Jan. 1996.

[2] D. D. Davis, T. K. Gaylord, E. N. Glytsis, and S. C. Mettler, "Very-high-temperature stable CO_2-laser induced long-period fibre gratings," *Electron. Lett.*, vol. 35, no. 9, pp. 740–742, 1999.

[3] G. Rego, O. Okhotnikov, E. Dianov, and V. Sulimov, "High-temperature stability of long-period fiber gratings produced using an electric arc," *J. Lightw. Technol.*, vol. 19, no. 10, pp. 1574–1579, Oct. 2001.

[4] G. Humbert and A. Malk, "Characterizations at very high temperature of electric arc-induced long-period fiber gratings," *Opt. Commun.*, vol. 208, no. 4–6, pp. 329–335, 2002.

[5] Y. Ma et al., "All-fiber strain sensor based on dual side V-grooved long-period fiber grating," *IEEE Sens. J.*, vol. 21, no. 4, pp. 21572–21576, Oct. 2021.

[6] X. Chen et al., "Sensitivity-enhanced strain sensor with a wide dynamic range based on a novel long-period fiber grating," *IEEE Sens. J.*, vol. 22, no. 4, pp. 3196–3201, Feb. 2022.

[7] S. K. Mishra, B. Zou, and K. S. Chiang, "Wide-range pH sensor based on a smart hydrogel-coated long-period fiber grating," *IEEE J. Sel. Topics Quantum Electron.*, vol. 23, no. 2, pp. 284–288, Mar./Apr. 2017.

[8] Y. Ma et al., "Sinusoidal-core long period fiber grating for refractive index measurement," *J. Lightw. Technol.*, vol. 40, no. 14, pp. 4903–4910, Jul. 2022.

[9] O. Koyama, M. Matsui, T. Kagawa, Y. Suzuki, K. Ikeda, and M. Yamada, "Low-cost optical fiber temperature-sensing system employing optical transceivers for ethernet and long-period fiber grating," *Appl. Opt.*, vol. 58, no. 9, pp. 2366–2371, 2019.

[10] A. Imada et al., "Temperature measurement range changeability of ethernet-based optical fiber sensing system using an optical attenuator," in *Proc. 26th Optoelectron. Commun. Conf.*, 2021, pp. 1–3.

[11] P. S. S. dos Santos, P. A. S. Jorge, J. M. M. M. de Almeida, and L. Coelho, "Low-cost interrogation system for long-period fiber gratings applied to remote sensing," *Sensors*, vol. 19, no. 7, 2019, Art. no. 1500.

[12] S. Alamandala, S. Prasad R.L.N., and R. K. Pancharathi, "Cost-effective load measurement system for health monitoring using long-period grating as an edge filter," *Opt. Fiber Technol.*, vol. 59, 2020, Art. no. 102328.

[13] Internet Control Message Protocol, 1981. [Online]. Available: https://www.rfc-editor.org/rfc/rfc792

[14] T. Murakami, O. Koyama, A. Kusama, M. Matsui, and M. Yamada, "Loss peak adjustment of long period fiber grating fabricated with CO_2 laser by applying tension," *IEICE Electron. Exp.*, vol. 15, no. 23, pp. 1–7, 2018.

[15] FORC-Photonics, Accessed: Nov. 2023. [Online]. Available: https://www.forc-photonics.ru/en/sensors_fbg/temperature_sensing/1/283/

[16] T&S, Accessed: Nov. 2023. [Online]. Available: https://www.China-tscom.com/products/fbg-sensor/

[17] M. Matsui, T. Murakami, O. Koyama, S. Takasuka, A. Kusama, and M. Yamada, "High temperature characteristic of LPFG fabricated with CO_2 laser under long-term heating," in *Proc. 22nd Optoelectron. Commun. Conf.*, 2017, pp. 1–2.